

Identification of p18^{INK4c} as a Tumor Suppressor Gene in Glioblastoma Multiforme

David A. Solomon,¹ Jung-Sik Kim,¹ Sultan Jenkins,¹ Habtom Ressom,¹ Michael Huang,² Nicholas Coppa,² Lauren Mabanta,¹ Darell Bigner,³ Hai Yan,³ Walter Jean,² and Todd Waldman¹

¹Lombardi Comprehensive Cancer Center, ²Department of Neurosurgery, Georgetown University School of Medicine, Washington, District of Columbia, and ³Department of Pathology, Duke University School of Medicine, Durham, North Carolina

Abstract

Genomic alterations leading to aberrant activation of cyclin/cyclin-dependent kinase (cdk) complexes drive the pathogenesis of many common human tumor types. In the case of glioblastoma multiforme (GBM), these alterations are most commonly due to homozygous deletion of p16^{INK4a} and less commonly due to genomic amplifications of individual genes encoding cyclins or cdks. Here, we describe deletion of the p18^{INK4c} cdk inhibitor as a novel genetic alteration driving the pathogenesis of GBM. Deletions of p18^{INK4c} often occurred in tumors also harboring homozygous deletions of p16^{INK4a}. Expression of p18^{INK4c} was completely absent in 43% of GBM primary tumors studied by immunohistochemistry. Lentiviral reconstitution of p18^{INK4c} expression at physiologic levels in p18^{INK4c}-deficient but not p18^{INK4c}-proficient GBM cells led to senescence-like G₁ cell cycle arrest. These studies identify p18^{INK4c} as a GBM tumor suppressor gene, revealing an additional mechanism leading to aberrant activation of cyclin/cdk complexes in this terrible malignancy. [Cancer Res 2008;68(8):2564–9]

Introduction

Glioblastoma multiforme (GBM) is the most lethal primary brain tumor. Approximately 10,000 GBMs are diagnosed each year in the United States, with an average survival of ~1 year. Activation of the epidermal growth factor signaling pathway by amplification and/or mutation of the epidermal growth factor receptor is found in most GBM tumors (1). Additionally, activation of the phosphatidylinositol-3-OH kinase signaling pathway via mutational inactivation of the PTEN tumor suppressor or mutational activation of the PIK3CA oncogene is also very common in GBM (2, 3). Finally, virtually all GBMs harbor genomic alterations that lead to the constitutive activation of cyclin-dependent kinases (cdk).

Several different genomic alterations are present in GBM tumors that lead to activation of cdks. A remarkable 60% to 80% of GBMs harbor homozygous deletions of the p16^{INK4a} tumor suppressor, which binds to and inhibits cdk4 and cdk6 (4, 5). Another 5% to 10% of GBMs have amplifications of individual cyclins and cdks, including cdk4, cdk6, and cyclin D1 (5–7). As such, it is by now

clear that aberrant activation of cdks is a particularly important genetic event contributing to the pathogenesis of GBM.

We have used high resolution single nucleotide polymorphism (SNP) arrays to interrogate the genomes of GBM samples in an effort to identify recurrent copy number alterations that may drive the pathogenesis of GBM. Using this approach, we have identified inactivation of the p18^{INK4c} cdk inhibitor as an additional genomic alteration that drives the pathogenesis of GBM.

Materials and Methods

Cell lines, xenografts, and primary tumors. Cell lines were obtained from the American Type Culture Collection (U87MG, U138MG, M059J, Hs683, H4, A172, LN18, LN229, CCF-STTG1, T98G, and DBTRG-05MG), DSMZ (8MGBA, 42MGBA, DKMG, GAMG, GMS10, LN405, and SNB19), and the Japan Health Sciences Foundation Health Science Research Resources Bank (AM38, NMC-G1, and KG-1-C). Normal human astrocytes (NHAs) were obtained from Clonetics and AllCells. All cell lines were grown in DMEM + 10% fetal bovine serum at 37° in 5% CO₂.

S.c. xenografts in immunodeficient mice were obtained from the Duke University Brain Tumor Center or created in the Lombardi Comprehensive Cancer Center Animal Shared Resource from tissue taken from patients undergoing craniotomy at Georgetown University Hospital (IRB #2006-344).

Snap-frozen primary GBM tumors and paired blood samples were obtained from the Brain Tumour Tissue Bank (London Health Sciences Centre) funded by the Brain Tumour Foundation of Canada. All tumors were graded by a neuropathologist as good or moderate on a scale of good to poor depending on the amount of tumor cells present (as opposed to hemorrhagic, necrotic, or fibrous tissue). All tumor samples were further categorized as “tumor center.”

Microarrays and bioinformatics. Genomic DNA derived from GBM cell lines and xenografts was interrogated with Affymetrix 250K Nsp I Human Gene Chip microarrays using protocols described by the manufacturer. Data processing was performed using dCHIP (8, 9). Additional details regarding the protocols used for data acquisition and processing, as well as the complete raw and processed data sets will be presented elsewhere.

PCR. Conventional PCR was performed using Taq Platinum (Invitrogen) as described by the manufacturer. qPCR was performed in an iCycler (Bio-Rad) using the Platinum Taq SYBR Green PCR Supermix (Invitrogen) according to the manufacturer's instructions. DNA copy number was calculated using the 2^{-Δ(ΔC_t)} method, normalizing to the copy number of an arbitrarily chosen region on chromosome 9 that was neither amplified nor deleted in the samples studied. All assays were performed at least in triplicate.

Western blot. Primary antibodies used were as follows: p18^{INK4c} clone DCS118 (Cell Signaling), p16^{INK4a} #554079 (BD-PharMingen), α-tubulin Ab-2 clone DM1A (Neomarkers), and cdk6 clone C-21 (Santa Cruz Biotechnology).

DNA sequencing. Individual exons of p18^{INK4c} were PCR amplified using conditions and primer pairs recently described by Sjoblom et al. (10). PCR products were purified using the Exo/SAP method followed by a Sephadex spin column. Sequencing reactions were performed using Big Dye v3.1 (Applied Biosystems) using an M13F primer, and analyzed on an Applied Biosystems 3730XL capillary sequencer. Sequences were analyzed using

Note: Supplementary data for this article are available at Cancer Research Online (<http://cancerres.aacrjournals.org/>).

Requests for reprints: Todd Waldman, Lombardi Comprehensive Cancer Center, Georgetown University School of Medicine, NRB E304, 3970 Reservoir Road, Northwest, Washington, DC 20057. Phone: 202-687-1340; Fax: 202-687-7505; E-mail: waldmant@georgetown.edu.

©2008 American Association for Cancer Research.
doi:10.1158/0008-5472.CAN-07-6388

Mutation Surveyor (Softgenetics). Traces with putative mutations were reamplified and sequenced from both tumor and matched normal DNA.

Immunohistochemistry. GBM tissue microarrays were obtained from US Biomax and contained 35 cases of GBM spotted in duplicate. Immunohistochemistry was performed using standard techniques using the same antibodies as for Western blot except using p16^{INK4a} antibody #554070 (BD-PharMingen). Antigen-antibody complexes were detected with the avidin-biotin peroxidase method using 3,3'-diaminobenzidine as the chromogenic substrate (Vectastain ABC kit; Vector Laboratories), and sections were counterstained with hematoxylin.

p18^{INK4c} lentivirus. A full-length, wild-type p18^{INK4c} cDNA (MGC 3907917) was obtained from Open Biosystems and cloned into the pCDF1-MCS2-EF1-Puro lentiviral expression vector backbone (System Biosciences). To make virus, this construct was cotransfected into 293T cells with pVSV-G (Addgene) and pFIV-34N (System Biosciences) helper plasmids using Fugene 6 (Roche) as described by the manufacturer. Virus-containing conditioned medium was harvested 48 h after transfection, filtered, and used to infect recipient cells in the presence of 8 µg/mL polybrene.

Flow cytometry. Cells were pulsed with 10 µmol/L BrdUrd for 1 h, trypsinized, and centrifuged. Cells were fixed and stained using the BrdUrd Flow kit (PharMingen) and analyzed by flow cytometry in a BD FACSort instrument using FCS Express v.3 software (DeNovo Software).

β-Galactosidase staining. Cells grown on coverslips were stained with the Senescence β-Galactosidase Staining kit (Cell Signaling) as described by the manufacturer.

Microscopy. All imaging was performed on an Olympus BX61 light microscope with a ×40 Plan-Apochromat objective.

Results

Homozygous deletion of p18^{INK4c} in GBM. In an effort to identify novel copy number alterations that drive the pathogenesis of GBM, we initially interrogated genomic DNA derived from 35 GBM cell lines and xenografts with Affymetrix SNP microarrays, as described in Materials and Methods. This analysis revealed focal deletions of chromosome 1p in 7 of 35 (20%) of samples (Fig. 1A).

This ~200- to 300-kb region of chromosome 1 contains two annotated genes—p18^{INK4c} and FAF1. p18^{INK4c} is a cdk inhibitor that binds to and inhibits cdk4 and cdk6, and is a known tumor suppressor in mice (11, 12). FAF1 binds to the intracellular domain of Fas and is a proapoptotic signal transduction molecule (13). To determine whether either of these genes was the likely target of the deletion, we examined the copy number information at individual probesets to identify the consensus region of deletion (Supplementary Fig. S1). This analysis revealed that three probesets were deleted in all samples studied, narrowing the consensus region of deletion to a 56- to 133-kb interval containing only p18^{INK4c}. These deletions of p18^{INK4c} were confirmed by PCR and qPCR analysis using primer pairs specific to p18^{INK4c} exon 1 (Supplementary Fig. S2; Fig. 1B). Finally, Western blot analysis showed the absence of p18^{INK4c} expression in GBM cells with confirmed homozygous deletions (Supplementary Fig. S3).

p18^{INK4c} deletions in primary tumor samples from the Cancer Genome Atlas. The NIH has recently sponsored a large-scale project to perform genomic analysis on GBM and other tumor types. As part of this project, they have recently released raw Affymetrix SNP microarray data on 106 primary GBM tumors. We analyzed these data with dCHIP to determine the copy number status of p18^{INK4c} in primary GBM tumors. As depicted in Fig. 1C, deletions of p18^{INK4c} were present in five tumors (5%). These deletions were not present in constitutional DNA from these patients studied with the same Affymetrix SNP microarrays (data not shown), demonstrating that the deletions are somatic. The available clinical and pathologic details of these samples are

presented in Supplementary Fig. S4. These data show that deletions of p18^{INK4c} are identifiable in uncultured primary human GBM samples, albeit at a lower apparent frequency than in our cultured samples.

Admixed nonneoplastic cells complicate the identification of p18^{INK4c} deletions in uncultured GBMs. We hypothesized that the lower apparent frequency of p18^{INK4c} deletions in uncultured GBM samples was due, at least in part, to the presence of admixed nonneoplastic human cells that are eliminated during *ex vivo* growth. To directly test this, we performed SNP microarray analysis on a primary GBM tumor and a matched first-passage xenograft that we derived from the tumor. Deletion of p18^{INK4c} was easily

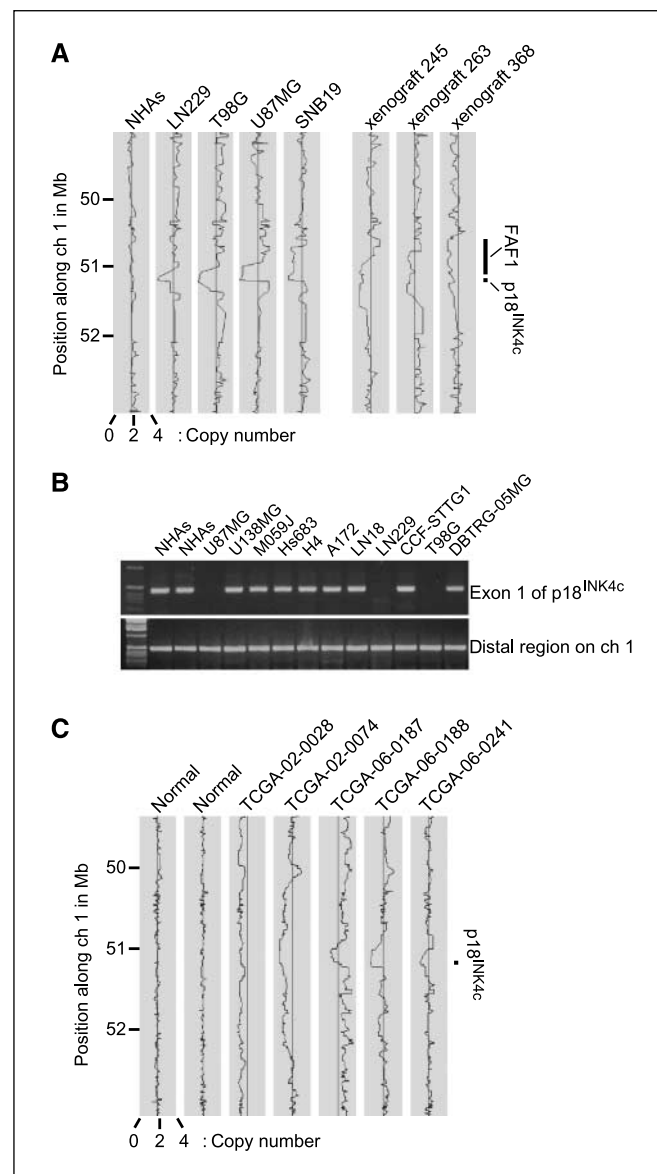


Figure 1. Homozygous deletions of p18^{INK4c} in GBM. **A**, copy number analysis of Affymetrix 250K SNP microarray data shows focal homozygous deletions of chromosome 1p in four GBM cell lines (*left*) and three GBM xenografts (*right*) but not in NHAs. **B**, PCR on genomic DNA derived from GBM cell lines confirms the presence of homozygous deletions in all four GBM cell lines with putative deletions (SNB19 not shown). **C**, copy number analysis of Affymetrix SNP microarray data shows p18^{INK4c} deletions in five uncultured primary GBM tumors. The raw SNP microarray data on the primary tumors was generated as part of The Cancer Genome Atlas.

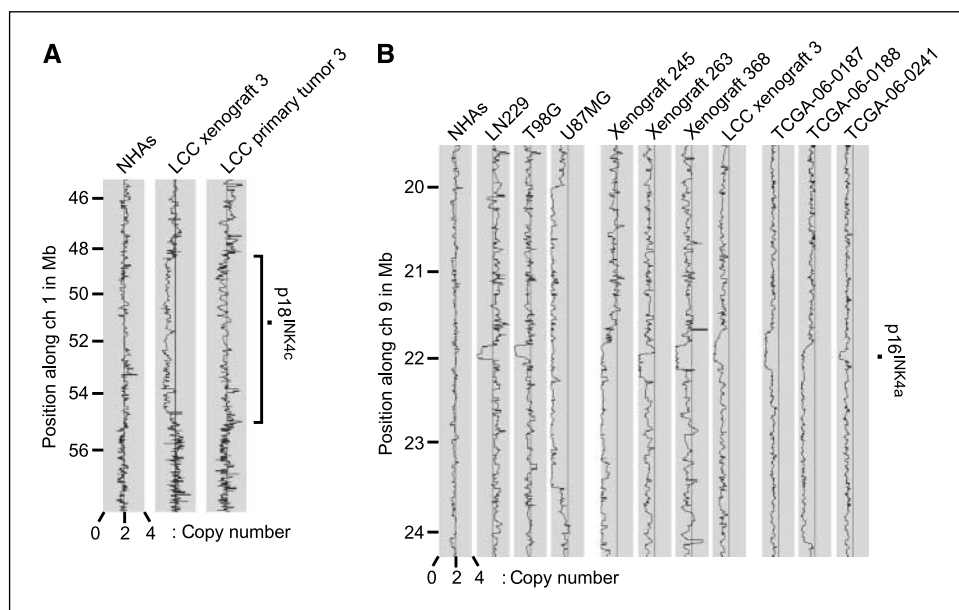


Figure 2. Heterogeneity of p18^{INK4c} deletions in GBM. *A*, copy number analysis of Affymetrix SNP microarray data shows deletion of p18^{INK4c} in a first-passage xenograft that is largely obscured by admixed normal cells in the primary tumor from which it was derived. *B*, copy number analysis of the p16^{INK4a} gene in cell lines (*left*), xenografts (*middle*), and primary tumors (*right*) harboring deletions of p18^{INK4c} reveals striking homogeneity with regard to p16^{INK4a} deletion in all sample types.

detectable in the first passage xenograft but was much less apparent (and would have been missed) in the primary tumor from which the xenograft was derived (Fig. 2A). This experiment clearly shows that the presence of admixed normal human cells is one factor that confounds the identification of p18^{INK4c} deletions in primary tumors. Xenograft growth eliminates admixed nonneoplastic human cells, enabling more efficient detection of p18^{INK4c} deletions with available technologies.

Heterogeneity of p18^{INK4c} deletion in GBM. Despite eliminating the influence of admixed nonneoplastic human cells by *ex vivo* growth, we did not observe *complete* copy number reduction at the p18^{INK4c} locus in either GBM xenografts or uncultured primary tumors (Fig. 1A and C). To determine whether this was an issue with sample quality or instead reflected a more fundamental underlying biology, we examined the copy number at the p16^{INK4a} locus in the same GBM samples that harbored deletions of p18^{INK4c}. Deletions of p16^{INK4a} were present in 12 of these 14 samples (86%). As expected, in cell lines, the copy number for *both* p16^{INK4a} and p18^{INK4c} was zero, reflecting the homogeneity of cultured cell lines (compare Fig. 2B to identical samples in Fig. 1A). In contrast, in more genetically heterogeneous xenografts and uncultured primary tumors, the copy number for p16^{INK4a} was near zero, whereas the copy number for p18^{INK4c} was 0.5 to 1.0 (compare Fig. 2B to identical samples in Fig. 1A and C). This analysis clearly shows that GBMs are homogenous with regard to p16^{INK4a} deletions and more heterogeneous with regard to p18^{INK4c} deletions.

Loss of p18^{INK4c} expression in GBM primary tumors. We next used immunohistochemistry to measure p18^{INK4c} expression in individual cells in primary GBM tumors. In particular, we measured the expression of p18^{INK4c} protein in 35 primary GBM specimens as part of a GBM tissue microarray (Fig. 3A). Remarkably, expression of p18^{INK4c} was completely lost in 15 of the 35 (43%) samples studied by immunohistochemistry (examples in *i* and *ii*). In samples expressing p18^{INK4c}, staining was primarily nuclear, with some cytoplasmic staining observable as has been reported by Bartkova et al. (14). By comparison, expression of p16^{INK4a} (known to be commonly deleted in GBM) was lost in 21 of the 35 (60%) samples studied (examples in *iii* and *iv*). Nine of the fifteen samples

(60%) lacking expression of p18^{INK4c} also lacked expression of p16^{INK4a}. Staining for α -tubulin was positive in all but one of the 70 tumor cores, demonstrating that all p18^{INK4c}-negative tumors were accessible for staining with other antibodies (example in *v*). This experiment showed that p18^{INK4c} expression is lost in ~40% to 50% of GBMs (Fig. 3B), and therefore, its inactivation is likely to play a major role in the pathogenesis of GBM.

Absence of p18^{INK4c} missense mutations in 82 GBM samples. We next sequenced p18^{INK4c} in 82 GBM samples lacking homozygous deletions, including 51 primary tumors, 14 xenografts, and 17 cell lines as described in Materials and Methods. The p18^{INK4c} coding region was wild-type in each of the 82 samples sequenced. Heterozygosity at a previously annotated synonymous SNP is depicted in Supplementary Fig. S5. This experiment showed that as for p16^{INK4a}, homozygous deletion of p18^{INK4c} is the predominant genetic mechanism leading to its inactivation during GBM pathogenesis.

Amplification of cdk6 in GBMs harboring intact p18^{INK4c} genes. Cdk6 is thought to be a particularly important target of inhibition by p18^{INK4c}, and Costello et al. (6) have previously described cdk6 amplifications in GBM samples. Therefore, we determined whether amplification of cdk6 might be present in our GBM samples with intact p18^{INK4c} genes. To test this, we first analyzed SNP microarray data and found amplifications of cdk6 in both a GBM cell line and xenograft with wild-type p18^{INK4c} (Supplementary Fig. S6A). Next, we expanded the analysis by using qPCR to measure cdk6 copy number in a panel of 51 GBM primary tumors and, in this way, identified an additional sample with cdk6 amplification (Supplementary Fig. S6B).

Lentiviral reconstitution of p18^{INK4c} expression in GBM cells leads to G₁ cell cycle arrest. To determine the phenotypic consequences of p18^{INK4c} deletion in GBM cells, we created a p18^{INK4c}-expressing lentivirus as described in Materials and Methods. Next, we infected five GBM cell lines-LN229, U87MG, T98G, SNB19 (each deleted for p18^{INK4c}), and M059J (wild-type p18^{INK4c}) with either empty vector or p18^{INK4c} virus. Infected cells were studied by Western blot (Fig. 4A), flow cytometry/BrdUrd incorporation (Supplementary Fig. S7; Fig. 4B), phase-contrast

microscopy (Fig. 4C), and staining for senescence-associated β -galactosidase activity (Fig. 4D).

Infection with the p18^{INK4c} lentivirus led to a physiologic level of expression, comparable with the endogenous levels of expression found in M059J GBM cells harboring an intact p18^{INK4c} gene (Fig. 4A). Importantly, ectopic expression of p18^{INK4c} led to a rapid and complete senescence-like G₁ cell cycle arrest in cells with homozygous deletions of p18^{INK4c} but not in cells with an intact p18^{INK4c} gene (Supplementary Fig. S7; Fig. 4B–D; data not shown). Interestingly, expression of p18^{INK4c} in p18^{INK4c}-deficient SNB19 cells led to rapid and complete cell death (Fig. 4C).

Discussion

Here, we identify p18^{INK4c} as a new GBM tumor suppressor gene by describing homozygous deletions in GBM cell lines, xenografts, and primary tumors, and complete loss of expression in 43% of GBMs studied by immunohistochemistry. Furthermore, we show that re-expression of p18^{INK4c} at physiologic levels in GBM cells that lack it leads to immediate senescent-like arrest in the G₁ phase of the cell cycle.

p18^{INK4c} is a member of the INK4 family of cdk inhibitors, which includes p16^{INK4a}, p15^{INK4b}, p18^{INK4c}, and p19^{INK4d}. Members of this family bind to cdk4 and cdk6 and inhibit their ability to bind to D-type cyclins, thereby inhibiting the formation of an active cdk/cyclin complex and leading to cell cycle arrest. Deletions at the

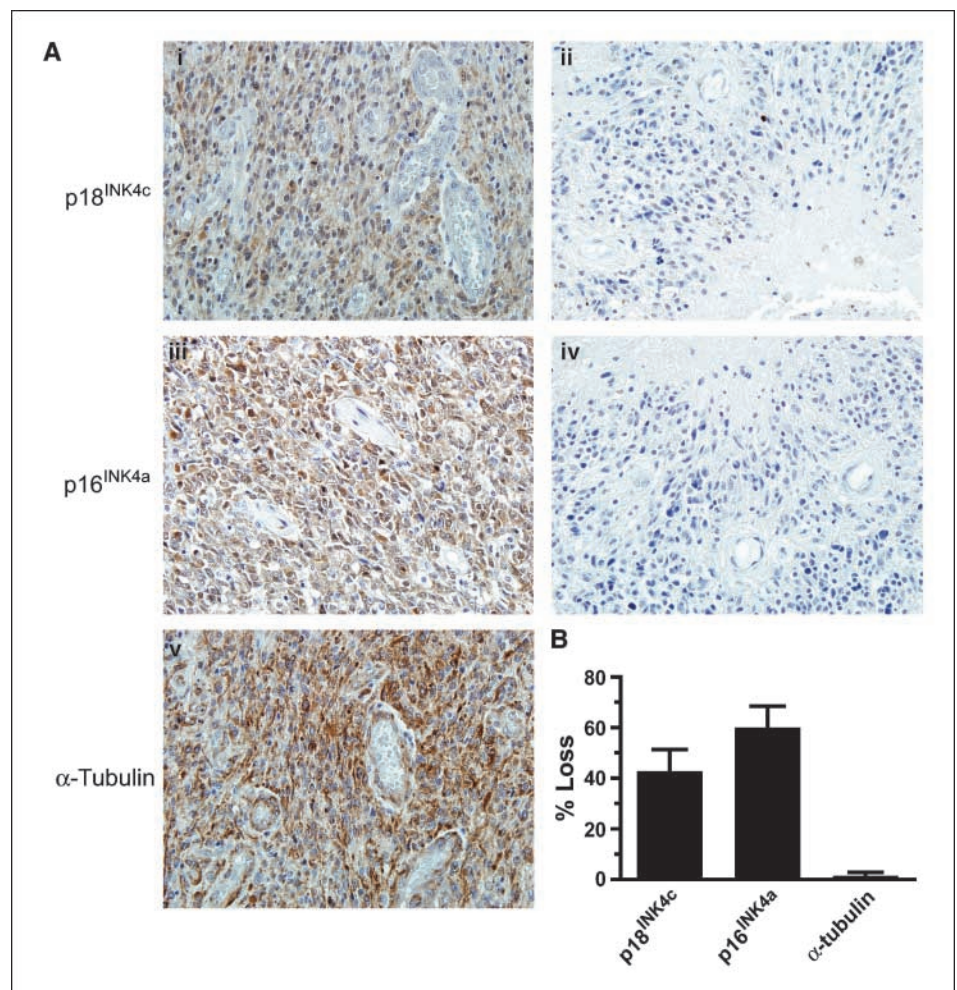
p18^{INK4c} locus have previously been implicated in the pathogenesis of other tumor types, including those of the brain (12, 15–18). Intriguingly, loss of both p18^{INK4c} and PTEN (both GBM tumor suppressors) has been shown to have synergistic effects on tumor formation in mice (19).

INK4 family members differ from each other in their patterns of expression and in the potency with which they bind individual cyclin/cdk complexes. p18^{INK4c} is thought to bind most potently to cdk6-specific complexes, although there is conflicting data on this point (11). The phenotypic consequences of binding to and inhibiting cdk4 and cdk6 with differing affinities are not well-understood.

We have shown that the presence of admixed nonneoplastic cells and intratumoral heterogeneity complicates the efficient identification of p18^{INK4c} deletions in uncultured primary tumors, using conventional technologies. However, it is also a formal possibility that the greater frequency of p18^{INK4c} deletions in cell lines and xenografts are artifacts of *ex vivo* culture.

It is also notable that the same GBM samples harboring *heterogeneous* deletions of p18^{INK4c} also often harbor remarkably *homogeneous* deletions of p16^{INK4a}. This finding was important as it enabled us to rule out issues of sample quality as a trivial explanation for our finding of heterogeneity. Furthermore, it suggests that homozygous deletion of p16^{INK4a} is an early event in the pathogenesis of GBM, whereas inactivation of p18^{INK4c} seems to occur later in the neoplastic process.

Figure 3. Loss of p18^{INK4c} expression in GBM primary tumors. Immunohistochemistry to GBM tissue microarrays was performed as described in Materials and Methods. A, representative GBMs that (i) express p18^{INK4c}, (ii) fail to express p18^{INK4c}, (iii) express p16^{INK4a}, and (iv) fail to express p16^{INK4a}. v, representative staining for α -tubulin. B, bar graph depicting the percentage of samples lacking expression of p18^{INK4c}, p16^{INK4a}, and α -tubulin.



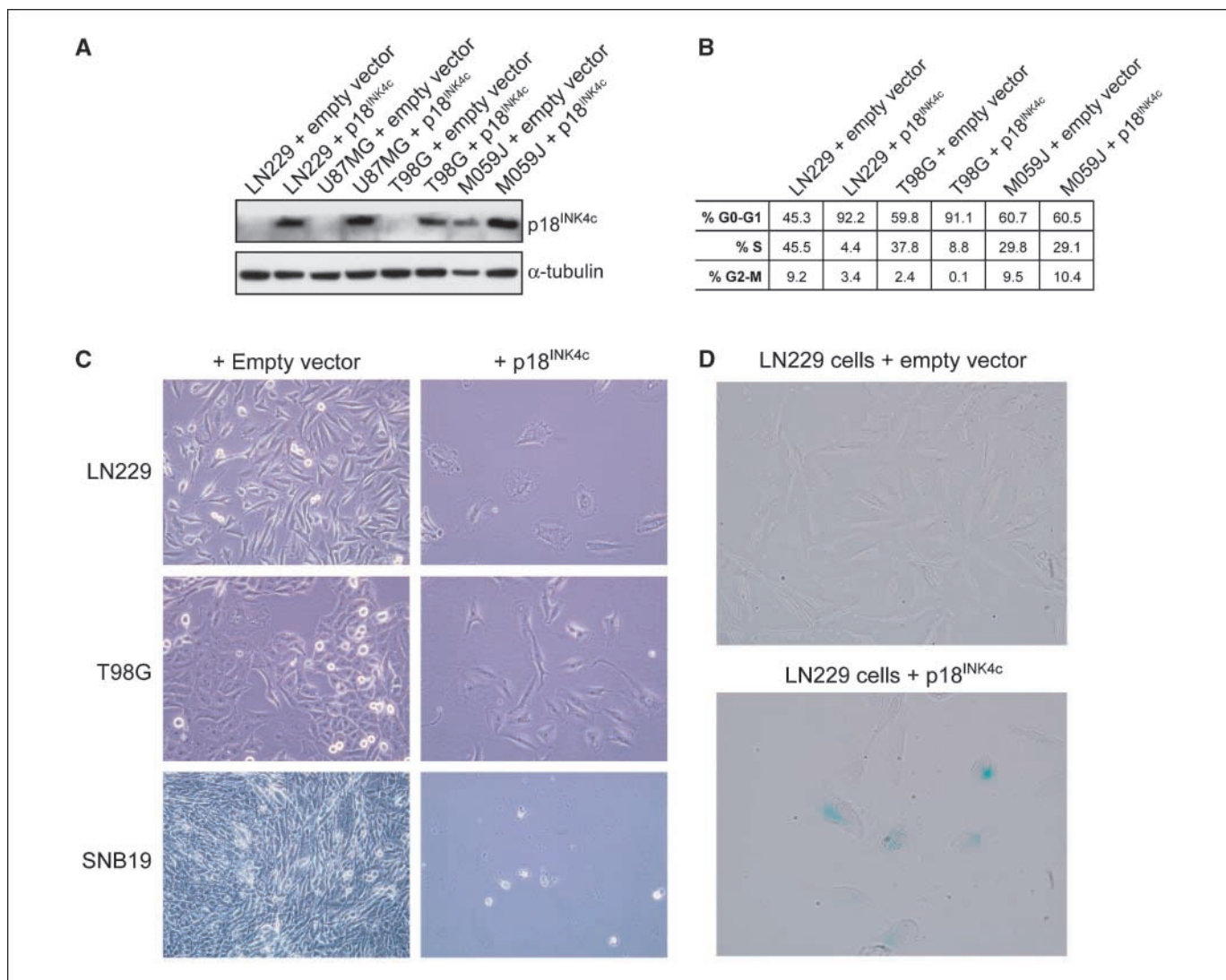


Figure 4. Reconstitution of p18^{INK4c} leads to senescence in GBM cells. **A**, Western blot for p18^{INK4c} 24 h postinfection shows lentiviral reconstitution of p18^{INK4c} expression in p18^{INK4c}-null LN229, U87MG, and T98G GBM cells (SNB19 not shown). The level of reconstituted expression is only slightly higher than the endogenous levels present in p18^{INK4c}-proficient M059J cells. **B**, cell cycle distributions 60 h postinfection with control or p18^{INK4c}-expressing lentiviruses. Infection with p18^{INK4c} lentivirus causes G₁ cell cycle arrest in p18^{INK4c}-deleted LN229 and T98G cells but not in p18^{INK4c}-proficient M059J cells. **C**, phase contrast microscopy of cells 7 d postinfection shows that reconstitution of p18^{INK4c} expression in p18^{INK4c}-deficient LN229 and T98G cells leads to morphologic changes resembling senescence, whereas expression of p18^{INK4c} in SNB19 cells leads to frank cell death. **D**, reconstitution of p18^{INK4c} expression in LN229 cells leads to induction of senescence-associated β-galactosidase activity. Similar results were observed in T98G cells but not in p18^{INK4c}-proficient M059J cells (data not shown).

p18^{INK4c} seems to be inactivated in GBM predominantly by homozygous deletion. This is similar to the situation for p16^{INK4a}, in which homozygous deletion is the major mechanism of inactivation in GBM (although point mutations in p16^{INK4a} also occur, albeit at a lower frequency; ref. 20). In the case of p16^{INK4a}, this has been rationalized by suggesting that there is selection pressure for loss of p14^{ARF} as well. It is possible that there is similar selection pressure for simultaneous codeletion of p18^{INK4c} and FAF1 (or an adjacent as yet uncharacterized gene or noncoding RNA) during the pathogenesis of GBM.

In summary, here we have identified p18^{INK4c} as a tumor suppressor gene that is genetically inactivated by homozygous deletion during the pathogenesis of GBM. Additional detailed studies are warranted to identify the phenotypic consequences of p18^{INK4c} deletion during the pathogenesis of GBM.

Acknowledgments

Received 11/28/2007; revised 1/24/2008; accepted 2/11/2008.

Grant support: Georgetown University School of Medicine (T. Waldman and W. Jean), a training grant T32-CA009686 from the National Cancer Institute, NIH (S. Jenkins), and the Lombardi Comprehensive Cancer Center is funded by P30-CA051008 from the National Cancer Institute, NIH.

The costs of publication of this article were defrayed in part by the payment of page charges. This article must therefore be hereby marked *advertisement* in accordance with 18 U.S.C. Section 1734 solely to indicate this fact.

We thank Michelle Lombard and Karen Cresswell for assistance with flow cytometry, Aaron Foxworth and Syid Abdullah for assistance with animal husbandry, Marcela White of the Brain Tumor Tissue Bank at the London Health Sciences Centre in Ontario, Canada for her assistance with the procurement of high quality GBM specimens, and Yarden Samuels for her comments on the manuscript.

The results published here are, in part, based on data generated by The Cancer Genome Atlas pilot project established by the National Cancer Institute and National Human Genome Research Institute. Information about The Cancer Genome Atlas and the investigators and institutions who constitute The Cancer Genome Atlas research network can be found at <http://cancergenome.nih.gov>.

References

1. Libermann TA, Nusbaum HR, Razon N, et al. Amplification, enhanced expression and possible rearrangement of EGF receptor gene in primary human brain tumors of glial origin. *Nature* 1985;313:144-7.
2. Rasheed BK, Stenzel TT, McLendon RE, et al. PTEN gene mutations are seen in high-grade but not in low-grade gliomas. *Cancer Res* 1997;57:4187-90.
3. Broderick DK, Di C, Parrett TJ, et al. Mutations of PIK3CA in anaplastic oligodendrogliomas, high-grade astrocytomas, and medulloblastomas. *Cancer Res* 2004;64:5048-50.
4. Jen J, Harper JW, Bigner SH, et al. Deletion of p16 and p15 genes in brain tumors. *Cancer Res* 1994;54:6353-8.
5. Schmidt EE, Ichimura K, Reifenberger G, Collins VP. CDKN2 (p16/MTS1) gene deletion or CDK4 amplification occurs in the majority of glioblastomas. *Cancer Res* 1994;54:6321-4.
6. Costello JF, Plass C, Arap W, et al. Cyclin-dependent kinase 6 (CDK6) amplification in human gliomas identified using two-dimensional separation of genomic DNA. *Cancer Res* 1997;57:1250-4.
7. Buschges R, Weber RG, Actor B, Lichter P, Collins VP, Reifenberger G. Amplification and expression of cyclin D genes (CCND1, CCND2, and CCND3) in human malignant gliomas. *Brain Pathol* 1999;9:435-42.
8. Li C, Wong WH. Model-based analysis of oligonucleotide arrays: expression index computation and outlier detection. *Proc Natl Acad Sci U S A* 2001;98:31-6.
9. Lin M, Wei LJ, Sellers WR, Lieberfarb M, Wong WH, Li C. dChipSNP: significance curve and clustering of SNP-array-based loss-of-heterozygosity data. *Bioinformatics* 2004;20:1233-40.
10. Sjoblom T, Jones S, Wood LD, et al. The consensus coding sequences of human breast and colorectal cancers. *Science* 2006;314:268-74.
11. Guan KL, Jenkins CW, Li Y, et al. Growth suppression by p18, a p16INK4/MTS1- and p14INK4B/MTS2-related CDK6 inhibitor, correlates with wild-type Rb function. *Genes Dev* 1994;8:2939-52.
12. Bai F, Pei XH, Godfrey VL, Xiong Y. Haploinsufficiency of p18(INK4c) sensitizes mice to carcinogen-induced tumorigenesis. *Mol Cell Biol* 2003;23:1269-77.
13. Chu K, Niu X, Williams LT. A Fas-associated protein factor, FAF1, potentiates Fas-mediated apoptosis. *Proc Natl Acad Sci U S A* 1995;92:11894-8.
14. Bartkova J, Thullberg M, Rajpert-De Meyts E, Skakkebaek NE, Bartek J. Cell cycle regulators in testicular cancer: loss of p18INK4C marks progression from carcinoma *in situ* to invasive germ cell tumours. *Int J Cancer* 2000;85:370-5.
15. Pohl U, Cairncross JG, Louis DN. Homozygous deletions of the CDKN2C/p18INK4C gene on the short arm of chromosome 1 in oligodendrogliomas. *Brain Pathol* 1999;9:639-43.
16. Kulkarni MS, Daggett JL, Bender TP, Kuehl WM, Bergsagel PL, Williams ME. Frequent inactivation of the cyclin-dependent kinase inhibitor p18 by homozygous deletion in multiple myeloma cell lines: ectopic p18 expression inhibits growth and induces apoptosis. *Leukemia* 2002;16:127-34.
17. Franklin DS, Godfrey VL, Lee H, et al. CDK inhibitors p18(INK4c) and p27(Kip1) mediate two separate pathways to collaboratively suppress pituitary tumorigenesis. *Genes Dev* 1998;12:2899-911.
18. Uziel T, Zindy F, Xie S, et al. The tumor suppressors Ink4c and p53 collaborate independently with Patched to suppress medulloblastoma formation. *Genes Dev* 2005;19:2656-67.
19. Bai F, Pei XH, Pandolfi PP, Xiong Y. p18Ink4c and PTEN constrain a positive regulatory loop between cell growth and cell cycle control. *Mol Cell Biol* 2006;26:4564-76.
20. Kyritsis AP, Zhang B, Zhang W, et al. Mutations of the p16 gene in gliomas. *Oncogene* 1996;12:63-7.

Supplemental Figure Legends

Supplemental Fig. 1. Identification of the Minimal Region of Deletion. Detailed analysis of SNP microarray probeset data reveals the common area of deletion on chromosome 1 to be 51.166 Mb to 51.222, which includes a single gene – p18^{INK4c}.

Supplemental Fig. 2. qPCR confirms copy number reduction of p18^{INK4c} in GBM samples. (A) Examples of qPCR traces from normal human astrocytes (NHAs) and two GBM samples for p18^{INK4c} exon 1 (top panel) and a region on chromosome 9 without copy number alteration (bottom panel). (B) Copy number estimate at the p18^{INK4c} locus by SNP microarray and qPCR analysis for NHAs and those GBM cell lines and xenografts with identified deletions of p18^{INK4c}.

Supplemental Fig. 3. Expression of p18^{INK4c} in GBM Cells. Western blots using antibodies to p18^{INK4c} confirms that each of the four cell lines with homozygous deletions of p18^{INK4c} fails to express p18^{INK4c} protein. All of the cell lines with deletions of p18^{INK4c} also fail to express p16^{INK4a}, demonstrating that inactivation of these related INK4 family members is not mutually exclusive during the pathogenesis of GBM.

Supplemental Fig. 4. Clinical and Pathological Details of The Cancer Genome Atlas Samples. Information available for the primary tumor samples harboring deletions of p18^{INK4c} is shown.

Supplemental Fig. 5. Sequencing of p18^{INK4c} in GBM Samples. Analysis of sequence traces from 51 primary tumors, 14 xenografts, and 17 cell lines revealed the presence of a common synonymous SNP present in both tumor and normal DNAs (shown) but no somatic or non-synonymous alterations.

Supplemental Fig. 6. Amplification of cdk6 in p18^{INK4}-Proficient GBM Cells and Tumors. (A) Copy number analysis of Affymetrix SNP microarray data demonstrates genomic amplifications of cdk6 in GBM xenograft 561 and cell line CCF-STTG1 but not in normal human astrocytes (NHAs). (B) qPCR confirms the amplifications in xenograft 561 and cell line CCF-STTG1, identifies an additional amplification in primary tumor 1118, and identifies several additional samples with copy number gains.

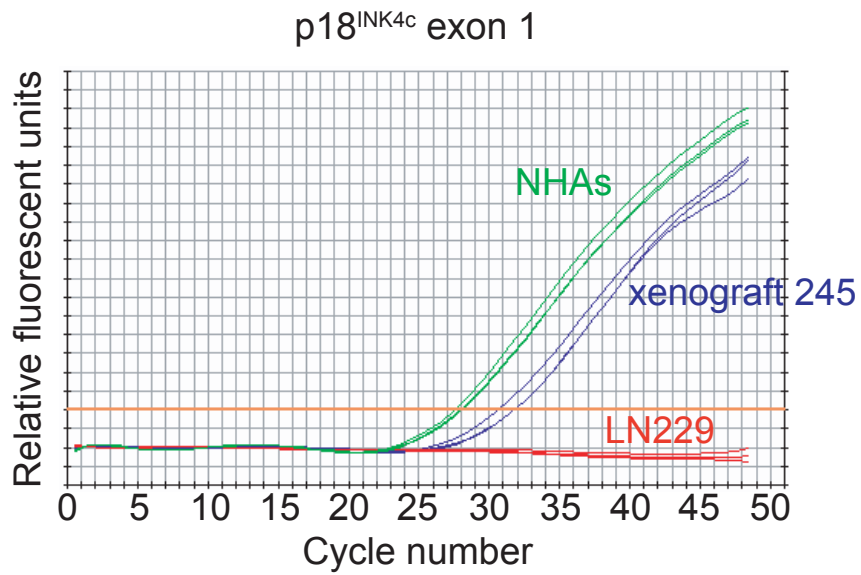
Supplemental Fig. 7. Reconstitution of p18^{INK4c} Leads to G1 Cell Cycle Arrest in GBM Cells. Flow cytometry 60 h. post-infection reveals that the p18^{INK4c} lentivirus causes G1 cell cycle arrest in p18^{INK4c}-deleted LN229 and T98G cells, but not in p18^{INK4c}-proficient M059J cells.

Supplemental Figure 1

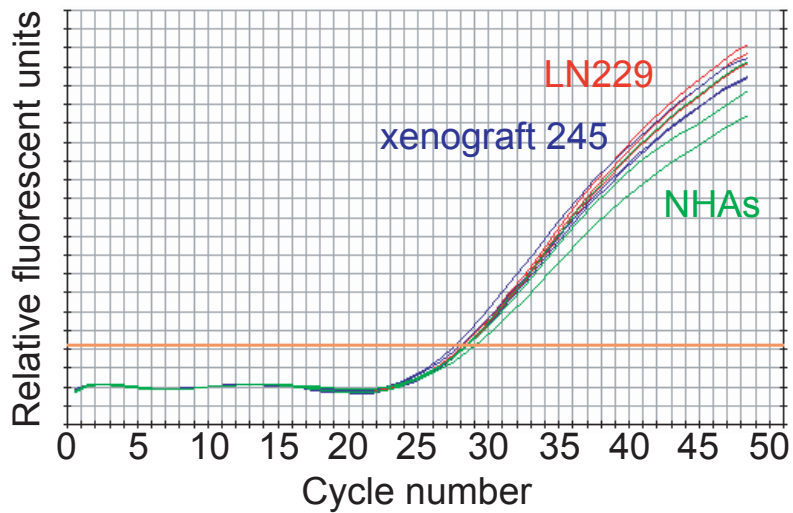
Marker	Position on				
	Ch 1 (Mb)	LN229	T98G	U87MG	SNB19
SNP_A-2163341	50.922	+	+	+	+
SNP_A-2310917	50.961	+	+	+	+
SNP_A-1869840	50.961	+	+	+	+
SNP_A-2281703	51.025	+	+	-	+
SNP_A-4218455	51.108	+	-	-	+
SNP_A-2092963	51.166	-	-	-	-
SNP_A-2123114	51.211	-	-	-	-
SNP_A-4226194	51.222	-	-	-	-
SNP_A-2080161	51.241	+	-	+	+
SNP_A-2042180	51.241	+	-	+	+
SNP_A-1917826	51.250	+	-	+	+
SNP_A-2192736	51.355	+	+	+	+
SNP_A-2064195	51.377	+	+	+	+

p18INK4c

A



chromosome 9 region without copy number alteration

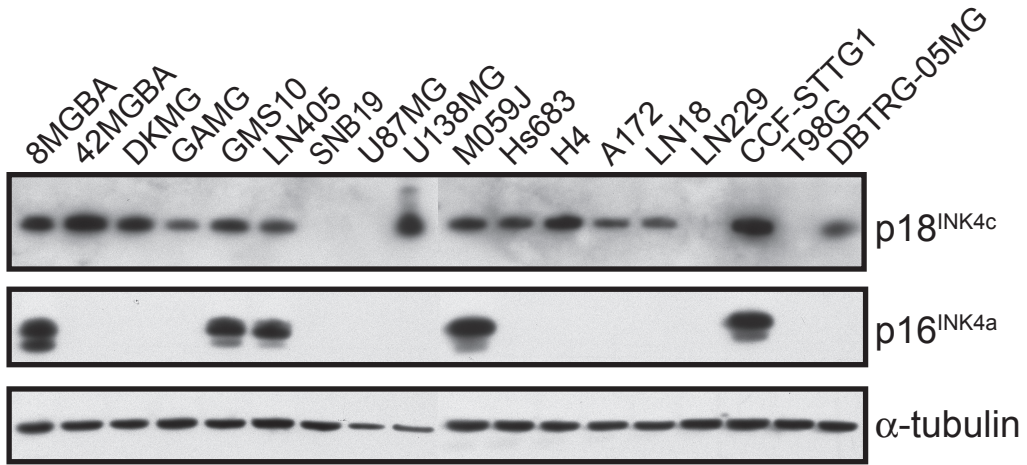


B

Copy number estimate at the p18^{INK4c} locus

Sample	SNP microarray	qPCR
NHAs	2.1	2.0 +/- 0.2
LN229	0.2	0.0 +/- 0.0
T98G	0.1	0.0 +/- 0.0
U87MG	0.0	0.0 +/- 0.0
SNB19	0.4	0.0 +/- 0.0
xenograft 245	0.7	1.0 +/- 0.1
xenograft 263	1.4	1.1 +/- 0.1
xenograft 368	0.9	0.2 +/- 0.0

Supplemental Figure 3



Supplemental Figure 4

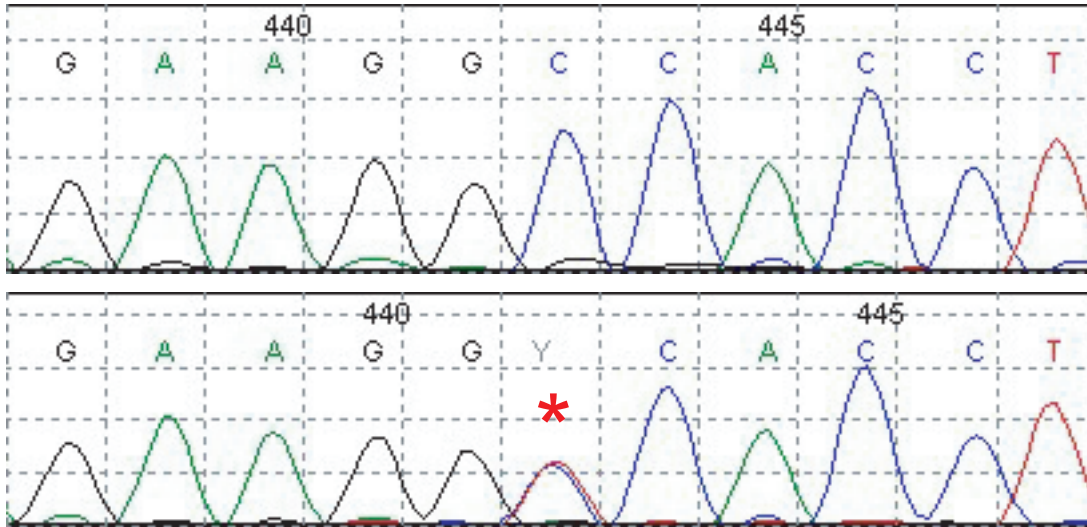
Tumor Sample	Location of Tumor	Patient Sex	Date of Birth	Date of Surgery	Date of Death
TCGA-02-0028	frontal lobe	male	4/12/1959	8/1/2005	10/14/2005
TCGA-02-0074	parietal lobe	female	8/11/1937	10/19/2005	8/25/2006
TCGA-06-0187	not listed	not listed	not listed	not listed	not listed
TCGA-06-0188	not listed	not listed	not listed	not listed	not listed
TCGA-06-0241	not listed	not listed	not listed	not listed	not listed

Tumor Sample	Tumor Section	% Tumor Cells	% Tumor Nuclei	% Normal Cells	% Necrosis	% Stromal Cells	% Leukocyte Infiltration	Cellularity	Endothelial Proliferation	Palisading Necrosis
	bottom	80-84	95-100	0	16-20	0	0	medium	yes	yes
TCGA-02-0074	top	80-84	95-100	0	16-20	0	0	low	no	yes
	bottom	95-100	95-100	0	1-5	0	0	low	no	no
TCGA-06-0187	top	90-94	95-100	0	6-10	0	0	medium	yes	no
	bottom	90-94	95-100	0	6-10	0	0	medium	yes	yes
TCGA-06-0188	top	80-84	95-100	0	6-10	6-10	0	low	yes	yes
	bottom	60-69	95-100	0	6-10	26-30	0	medium	yes	yes
TCGA-06-0241	top	95-100	95-100	0	1-5	0	0	high	yes	yes
	bottom	90-94	95-100	0	6-10	0	0	high	yes	yes

Supplemental Figure 5

sequence traces of p18^{INK4c} exon 2

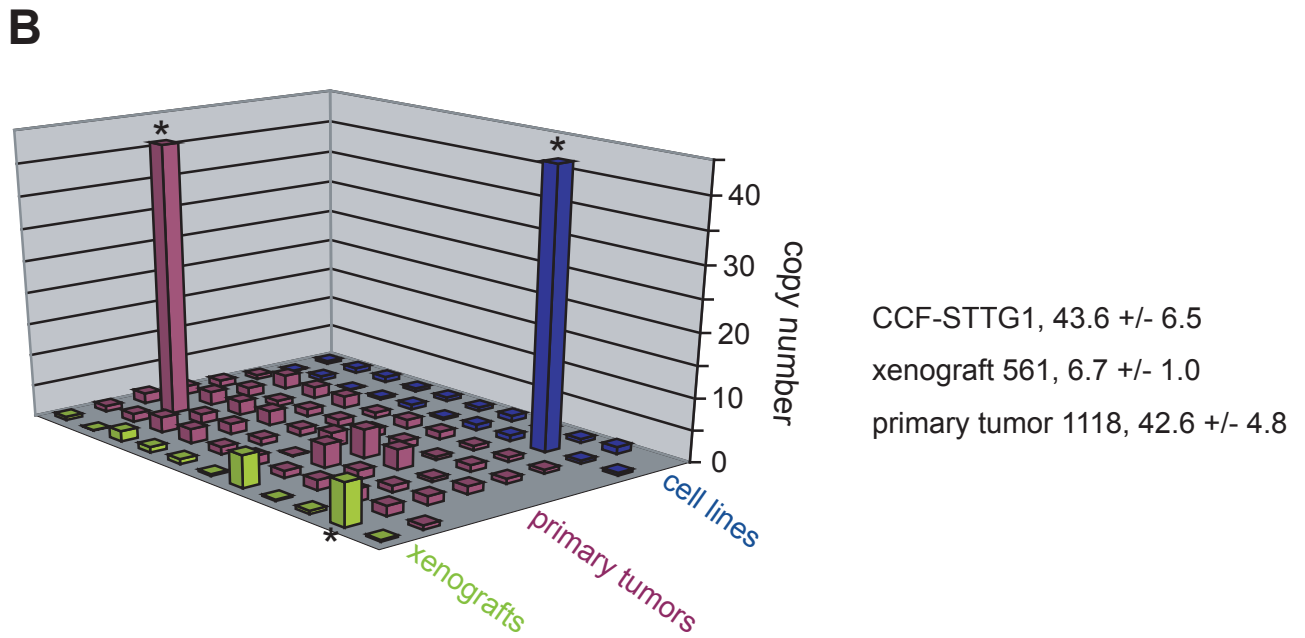
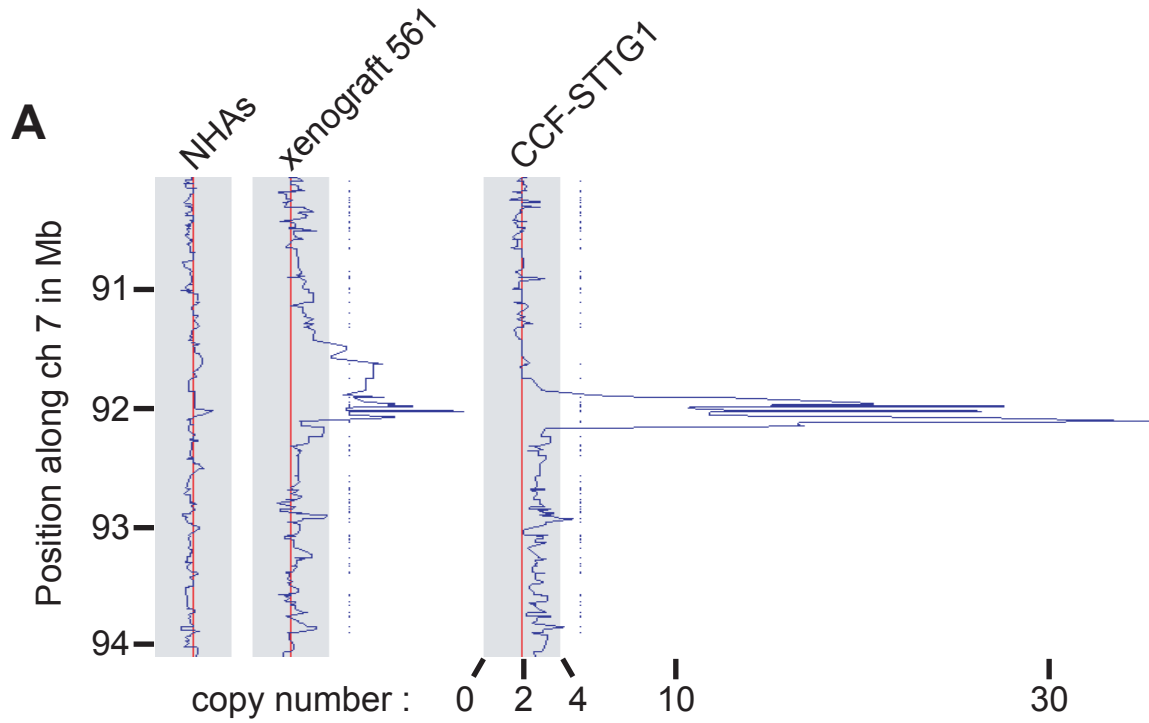
base 5912, Gly114



primary tumor 1209
homozygous C/C

primary tumor 785
heterozygous C/T

Supplemental Figure 6



Supplemental Figure 7

